

Generation of the current normal to the surface of antenna by electromagnetic waves and its application in the high responsive receiver

V.N. Dobrovolsky

V. Lashkaryov Institute of Semiconductor Physics, NAS of Ukraine, 03680 Kyiv, Ukraine
E-mail: sizov@isp.kiev.ua

Abstract. Generation of the initial current normal to the surface of antenna by electromagnetic waves has been considered. It has been shown that the angle of grazing (or sliding) for the wave with the electric vector in the plane normal to the surface varies the radiation resistance over a wide range. This property allows matching the radiation impedances and loads. Here, it has been proposed to use this property to create a highly-sensitive radiation detector. In relation with this task, a model of the radiation detection of the input radiation signal by a direct quadratic detector in the stationary mode with the diode included as the load has been considered. The obtained results prove that a diode with the high differential resistance can effectively operate with the antenna. The rise of the resistance increases the detector response voltage, its responsivity, and decreases the receiver noise equivalent power. Improvement of these characteristics by orders of magnitude is possible. The considered mechanism allows detectors to operate in the infrared spectral range, and the increase in the wavelength, in principle, does not limit its functioning.

Keywords: matching the radiation impedances and loads, quadratic detector, high responsivity, low NEP, Schottky diode.

<https://doi.org/10.15407/spqeo24.01.076>
PACS 07.50.Hp, 84.40.Ba, 85.30.Kk

Manuscript received 01.05.20; revised version received 24.12.20; accepted for publication 10.02.21; published online 09.03.21.

1. Introduction

In electromagnetic radiation receivers with an antenna, radiation generates current in the antenna and creates the energy flux into its load. If an incidence of the radiation is not normal, the current has tangential and normal surface antenna components. Usually, the first from them is applied [1]. By contrast, in this paper, application of the normal current is discussed.

It is shown that the grazing angle of the wave varies the radiation resistance over a wide range. Due to this, it is possible to realize the full matching the radiation with different loads, at which all energy incident on the antenna enters into them. This property is proposed to be used in the high responsive receivers.

A detector is a known type of antenna load. In this case, the responsivity and noise equivalent power (NEP) are main figures of merit for the receiver. They define the minimum signal power that it can detect when suppressing external noise. In the paper, a model of direct quadratic detection of an input signal with a load diode in a stationary mode is constructed. It showed that a diode with a high differential resistance can effectively

operate with the antenna in question. The rise of this resistance increases the voltage of its response and responsivity, and decreases the NEP of receiver. They improve its performances by orders of magnitude.

The features of the receiver considered in this paper are as follows. A metal plate of a simple shape operates as an antenna. A plane wave, period of which is much longer than the Maxwell relaxation time in the antenna, obliquely falls on its surface. Therefore, the normal to surface antenna component of this wave electric field and the respective field of reflected wave both induce space charge under the surface. Its change in time generates initial current, which charges the opposite surface of the antenna, and creates current in the load connected between it and the ground. The antenna thickness is much greater than the length of the Debye screening, therefore, the bulk of the antenna is neutral, this surface is equipotential, and only the capacitance between it and the ground defines the reactive component of the antenna impedance. The inductance of the load is used to match it and the antenna.

The numerical calculations presented in the examples are performed for the wavelength $3 \cdot 10^{-3}$ m.

This length is included in the actively studied THz/sub THz frequency range and is close to the wavelength of Internet [2, 3]. In the calculations, the characteristics of the Schottky diodes and tunneling ones, described in the literature, have been taken.

The proposed method for improving the properties of receivers can be used, starting from the infrared range, and increasing the wavelength, in principle, does not limit it.

Fig. 1 displays the named receiver design features. They will be considered below.

2. Matching the radiation with the load of antenna

The conditions for matching the radiation with the antenna load were derived as based on the laws of charge and energy conservation.

2.1. Induced current I_{ind}

The wave falls obliquely onto the surface of the antenna and is reflected (top of Fig. 1a). Its electric field $\mathbf{E}_i(E_{ix}, 0, E_{iz})$ is

$$\mathbf{E}_i = \mathbf{E}_i^0 \cdot \cos(\omega t - k_x x - k_z z). \quad (1)$$

Here, $\mathbf{E}_i^0(E_{ix}^0, 0, E_{iz}^0)$ is the field amplitude, ω – circular frequency, t – time, $\mathbf{k}(k_x, 0, k_z)$ – wave vector, $Oxyz$ is the Cartesian coordinate system. The following relationships will be used: wave period $T = 2\pi/\omega$, frequency $\nu = 1/T$, $k_x = k \cos \nu$, $k_z = k \sin \nu$, module $|\mathbf{k}| = k = \sqrt{k_x^2 + k_z^2} = 2\pi/\lambda$, $\omega = ck/\sqrt{\epsilon_e \mu_e}$, $c = 1/\sqrt{\epsilon_0 \mu_0}$, where ν is the grazing angle of a wave, λ – wavelength, ϵ_e – relative permittivity, μ_e – relative magnetic permeability in the external dielectric over the antenna, c – speed of light in vacuum, ϵ_0 and μ_0 – electric and magnetic constants. The value $c/\sqrt{\epsilon_e \mu_e}$ is the wave velocity in the dielectric and $(c/\sqrt{\epsilon_e \mu_e})$, $\tau_M = \epsilon_0 \epsilon_m / \sigma$, σ , ϵ_m and μ_m are the wave velocity, Maxwell relaxation time, conductivity, relative permittivity, and relative magnetic permeability in the metal, respectively.

The model assumes that λ , a and b are much greater than the length of the Debye screening in the antenna L_D , and neglects the edge effects at its boundaries. The grazing angles of waves and k_x are the same when falling and reflecting [4, 5]. Exp. (1) defines the field of the reflected wave after replacing “ i ” → “ r ” and $k_z \rightarrow -k_z$. The electric fields \mathbf{E}_i and \mathbf{E}_r lie in the plane of incidence, and the corresponding magnetic fields $\mathbf{H}_i(0, H_{iy}, 0)$ and $\mathbf{H}_r(0, H_{ry}, 0)$ are normal to it,

$$T \gg \tau_M. \quad (2)$$

The antenna is much thicker than L_D . The components E_{iz} and E_{rz} of the electric fields that are normal to the irradiated surface, induce the charge Q_{ind}

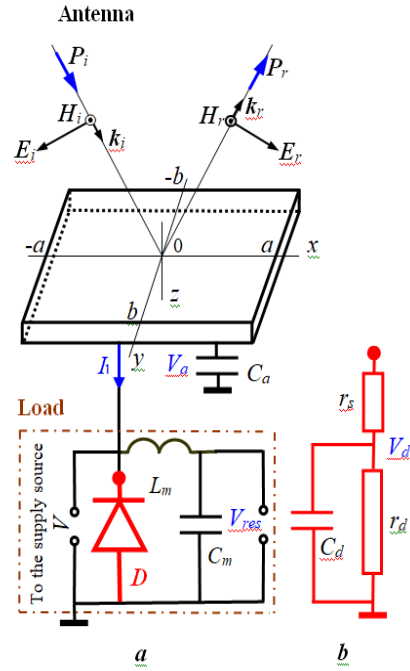


Fig. 1. a) The incidence of an electromagnetic wave on the antenna and its connection to the ground. The radiation generates current I_i and voltages V_a , V_d , and V_{res} . b) The equivalent circuit of detector D .

under it and current $I_{ind} = -\partial Q_{ind} / \partial t$ in the antenna bulk, charge Q_{ind}^* on the opposite surface and current I_{load} in the load. In this case, the inequality (2) ensures neutrality of the antenna bulk [5].

The relation $I_{load} = I_{ind} - (\partial Q_{ind}^* / \partial t)$ follows from conservation of charge, where $\partial Q_{ind}^* / \partial t$ is the bias current from the antenna, when neglecting the contribution of the side surfaces. If the distance between the antenna and ground is much smaller than λ , it is possible to use the antenna voltage V_a relatively to the ground and its capacitance C_a . The current

$$\partial Q_{ind}^* / \partial t = C_a (\partial V_a / \partial t) \text{ and}$$

$$I_{load} = I_{ind} - C_a (\partial V_a / \partial t). \quad (3)$$

Integration of the surface charge density $-\epsilon_0 \epsilon_e (E_{iz}|_{z=0} + E_{rz}|_{z=0})$ over $2a \cdot 2b$ gives Q_{ind} and

$$I_{ind} = I_0 \cdot \sin(\omega t), \quad (4)$$

where $I_0 = I_{i0} + I_{r0}$,

$$I_{i0} = -4c \epsilon_0 \sqrt{\frac{\epsilon_e}{\mu_e}} \frac{b \sin(ka \cos \nu)}{\cos \nu} E_{iz}^0, \quad (5)$$

and substitution “ i ” → “ r ” in (5) gives I_{r0} .

2.2. Powers of fluxes inherent to incident $\langle W_i \rangle$ and reflected $\langle W_r \rangle$ radiation, and also power $\langle W_l \rangle$ in the antenna load

The time-averaged quantity v equals $\langle v \rangle = \int_0^T v(t) dt / T$.

The module of Poynting's vector of incident wave (1) equals $\langle P_i \rangle = \langle u_i \rangle \cdot (c / \sqrt{\epsilon_e \mu_e})$, where $\langle u_i \rangle = \epsilon_0 \epsilon_e |\mathbf{E}_i^0|^2 / 2$ is the energy density [5], and

$$\langle W_i \rangle = 4ab \langle P_i \rangle \cdot \sin \nu. \quad (6)$$

After replacing “ i ” \rightarrow “ r ” in $\langle P_i \rangle$, $\langle u_i \rangle$ and $\langle W_i \rangle$, this expression sets the power $\langle W_r \rangle$.

For the low power $\langle W_i \rangle$, the admittance $Y = G + iB$ between the antenna and ground was introduced, where G and B are its active and reactive components, respectively, and i is the imaginary unity. The current

$$I_{\text{ind}} = -I_0 \text{Re} \left(i e^{i\omega t} \right) \quad (4)$$

creates the voltage $V_a = \text{Re} \dot{V}_a$ on the antenna, where $V_a = \text{Re} \dot{V}_a$, and power $\langle W_l \rangle = \langle I_{\text{ind}} V_a \rangle$ in the load,

$$\langle W_l \rangle = \frac{I_0^2 G}{2(G^2 + B^2)} \quad [6]. \quad (7)$$

2.3. Coefficient of matching the radiation and antenna load

The substitution $\langle W_i \rangle$, $\langle W_r \rangle$ and $\langle W_l \rangle$ with (5), into the condition of conservation of energy $\langle W_i \rangle = \langle W_l \rangle + \langle W_r \rangle$ and the introduction of the conductivity of the incident radiation $\Sigma_i = I_{i0}^2 / (2 \langle W_i \rangle)$,

$$\Sigma_i = 4c \epsilon_0 \sqrt{\frac{\epsilon_e}{\mu_e}} \frac{b \sin^2(ka \cos \nu)}{a \sin \nu}, \quad (8)$$

gave the relation:

$$E_{rz}^0 / E_{iz}^0 = (G^2 + B^2 - G \Sigma_i) / (G^2 + B^2 + G \Sigma_i).$$

Using it, the coefficient of matching the radiation and antenna load becomes $\eta = \langle W_l \rangle / \langle W_i \rangle$,

$$\eta = \frac{4}{\kappa + 2 + (1/\kappa)} \quad (9)$$

was deduced, in which $\kappa = (G^2 + B^2) / (G \Sigma_i)$.

If $\kappa = 1$, the coefficient $\eta = 1$, and agreement is complete. The selection of the load equality $B = 0$ can be implemented (see Section 3.3). Then the condition of complete agreement is simplified to $\Sigma_i = G$. From the latter, it immediately follows that the wide limits of the change in conductivity Σ_i provide the same ones in the conductivity G .

The inequality $B \neq 0$ does not change the situation, but increases the range of the necessary values Σ_i . In this case, each G corresponds to two B values with equal modules, but with different signs.

The model operates with the conductivity Σ_i , the radiation resistance is equal to the value $1/\Sigma_i$. The value η differs from the entered power ratio in the load and antenna [7].

2.4. Radiation conductivity

The two-dimensional plot at the bottom of Fig. 2 demonstrates that, if at the given grazing angle ν the size a rises, Σ_i/b (8) oscillates with the period $(\lambda/2)/\cos \nu$ and is damped. It is the largest at $a = a_{\text{max}} = 0.185\lambda/\cos \nu$, which is close to $(\lambda/4)/\cos \nu$. The three-dimensional plot in the figure shows that for any a value, Σ_i/b rises, if ν is reduced.

Σ_i deduction is based on the ratio $I_{\text{ind}} = -\partial Q_{\text{ind}} / \partial t$. It is correct, when during one period the radiation penetrates into the antenna deeper than the Debye length L_D . That is, the inequality $\left[(c / \sqrt{\epsilon_m \mu_m}) \cdot \sin \nu_m \right] \cdot T \gg L_D$ must be satisfied. Here, ν_m is the sliding angle in the metal, and the square brackets correspond to the speed of propagation inherent to radiation normal to its surface. For small angles ν and also if the values ϵ_e , μ_e are close to ϵ_m , μ_m , respectively, this inequality transforms into $\nu \gg L_D / \lambda$. Substitution $\nu = L_D / \lambda$ and $a = a_{\text{max}}$ in Exp. (8) defines the boundary of the Σ_i (8) validity: $\Sigma_i \ll \Sigma_i^b \approx 18.2c \epsilon_0 \sqrt{\epsilon_e / \mu_e} b / L_D$.

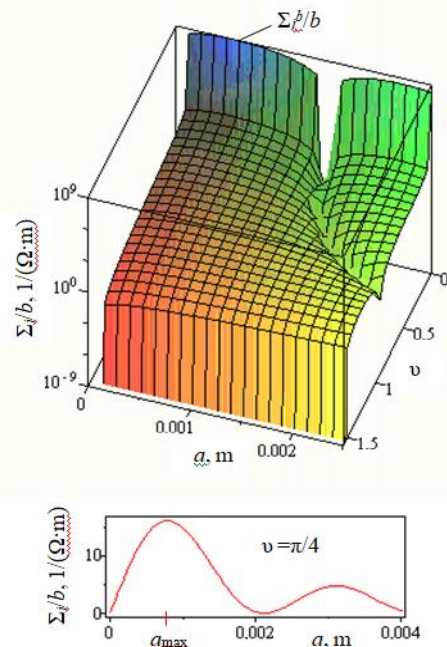


Fig. 2. At the bottom of the figure, the dependence Σ_i/b on the size a of the antenna for the grazing angle $\nu = \pi/4$ is placed, where Σ_i (8) is the conductivity of the incident radiation. The three-dimensional plot is the dependence Σ_i/b on a and ν . When plotting, it was accepted $\epsilon_e = \mu_e$, $\lambda = 3 \cdot 10^{-3}$ m and $L_D = 5 \cdot 10^{-11}$ m [11].

2.5. The variation of radiation conductivity over a wide range

The angle ν changes the conductivity Σ_i by orders of magnitude. It can be qualitatively explained as follows. Both relations $j_{mx} = -\partial H_{my}/\partial z$ and $j_{mz} = \partial H_{my}/\partial x$ follow from the Maxwell equation $\nabla \times \mathbf{H}_m = \mathbf{j}_m$ in the antenna, where \mathbf{H}_m and \mathbf{j}_m are the magnetic field and conduction current density, respectively.

The field $H_{my} \sim \exp(-z/d_{sc})$, where d_{sc} is the thickness of the skin layer [5]. On the other hand, the incident wave (1) defines the dependence of H_{my} on x in the form of the harmonic function $k \cos \nu \cdot x$. The relations $j_{mx} \sim 1/d_{sc}$ and $j_{mz} \sim k \cos \nu$ follow from these dependences. When changing the angle ν , the wide range of changes in j_{mz} causes similar ranges for current I_{i0} (5) and $\Sigma_i \sim I_{i0}^2$.

The situation is significantly different from that in an antenna with the tangential initial current. There, due to the small d_{sc} values, H_{my} sharply decreases with rising z , and this makes it difficult to implement the wide range of changes in the radiation conductivity.

3. Detector in the antenna load

3.1. Power in the active part of the detector $\langle W_d \rangle$

Fig. 1b shows the diode D equivalent circuit in the load. It has the active (detecting) part: differential resistance r_d and capacitance C_d , and also intrinsic series resistance r_s . For example, in a Schottky diode, this is the energy barrier and the resistance of the base, respectively. The impedance of active part is $Z_d = r_d + 1/(iC_d \omega)$. The

current through the detector $I_d = \text{Re} \left[\dot{V}_a / (r_s + Z_d) \right]$

creates the voltage $V_d = \text{Re} \left[\dot{V}_a Z_d / (r_s + Z_d) \right]$ and

power $\langle W_d \rangle = \langle I_d V_d \rangle$ on the active part,

$$\langle W_d \rangle = \frac{\eta \langle W_i \rangle}{1 + (r_s C_d \omega)^2} \frac{1}{r_d G}. \quad (10)$$

Since $r_d \gg r_s$ in the detectors, for simplicity, here and below the sum $r_d + r_s$ was replaced with r_d .

3.2. Responsivities of the detector R_{vd} and receiver R_v

The supply source (Fig. 1a) sets in the diode voltage-current characteristic $I(V)$ the operating voltage V_{op} and current I_{op} , where I is the total current through the diode, and V is the voltage across it.

The current I_d generated by radiation is

$$I_d = \frac{V_d}{r_d} + \beta V_d^2, \quad (11)$$

where $r_d = 1/(dI/dV)|_{V=V_{op}}$ and the coefficient of non-linearity $\beta = (d^2 I/dV^2)|_{V=V_{op}}/2$. The quadratic term causes the direct current $\beta \langle V_d^2 \rangle$. If it flows only through the resistance r_d , then the detector response voltage equals $V_{res} = \beta \langle V_d^2 \rangle r_d$. Because $\langle V_d^2 \rangle = \langle W_d \rangle r_d$, the responsivity of the active part of detector equals $R_{vd} = |V_{res}|/\langle W_d \rangle = |\beta| r_d^2$.

In the common case $\langle W_d \rangle \leq \langle W_i \rangle$, because of incomplete matching the radiation with load, and losses in it, $R_v \leq R_{vd}$. The equal signs take place in their absence. Then, the responsivity of the receiver R_v is as high as possible for the used diode.

Exp. (10) allows one to get $R_v = \eta R_{vm}$, where

$$R_{vm} = \frac{|\beta|}{1 + (r_s C_d \omega)^2} \cdot \frac{r_d}{G} \quad (12)$$

is the responsivity R_v , if full matching the radiation with load takes place.

3.3. Components G and B of the admittance Y between antenna and ground

Let us assume that in the load (Fig. 1a) the resistances of the supply source and voltmeter measuring V_{res} are high, and they do not contribute into Y . The inductance L_m is used for matching the radiation with load. The capacitance C_m connects it to the ground. Parasitic capacitances at the inputs of the detector and voltmeter are connected in parallel with the capacitances C_d and C_m , respectively, and are summed with them. They will not be recorded separately.

It was deduced:

$$G = \frac{1 + r_d r_s (C_d \omega)^2}{1 + (r_s C_d \omega)^2} \cdot \frac{1}{r_d} + \frac{r_m}{r_m^2 + \left(L_m \omega - \frac{1}{C_m \omega} \right)^2},$$

$$B = C_i^* \omega - \frac{L_m \omega - \frac{1}{C_m \omega}}{r_m^2 + \left(L_m \omega - \frac{1}{C_m \omega} \right)^2} - C_m \omega, \quad (13)$$

where r_m is an active resistance of the inductance L_m and

$$C_i^* = C_d + \left\{ C_d / \left[1 + (r_s C_d \omega)^2 \right] \right\} + C_m. \quad (14)$$

Table. Experimental characteristics of the diodes [7-10]

Diode	1	2	3	4
Parameter				
r_d, Ω	$8.6 \cdot 10^2$	$5.0 \cdot 10^4$	$3.2 \cdot 10^6$	$3.1 \cdot 10^{10}$
$C_d, 10^{-15} \text{ F}$	20	17	0	0
r_s, Ω	3	10	0	0
$\beta, \text{ A/V}^2$	$9.2 \cdot 10^{-3}$	$5.4 \cdot 10^{-4}$	$4.7 \cdot 10^{-7}$	$4.9 \cdot 10^{-10}$
$R_{vm}, \text{ V/W}$	$4.8 \cdot 10^3$	$2.3 \cdot 10^4$	$4.8 \cdot 10^6$	$4.8 \cdot 10^{11}$
NEP, W	$7.8 \cdot 10^{-13}$	$1.2 \cdot 10^{-12}$	$4.8 \cdot 10^{-14}$	$8.3 \cdot 10^{-17}$
NEP _{ph} , W	$1.1 \cdot 10^{-11}$	$3.5 \cdot 10^{-12}$	$5.9 \cdot 10^{-14}$	$8.4 \cdot 10^{-17}$
$L_{m0}, 10^{-11} \text{ H}$	3.0	3.1	3.8	3.8
Source	[7]	[8]	[9]	[10]

If $L_m = L_{m0}$, where

$$L_{m0} = \frac{1}{\omega^2} \left\{ \frac{1 + \sqrt{1 - 4[r_m(C_i^* - C_m)\omega]^2}}{2(C_i^* - C_m)} + \frac{1}{C_m} \right\}, \quad (15)$$

the equality $B = 0$ is valid. Its appearance is related with the resonance of currents in the oscillatory contour that it formed by the inductance L_m and capacitances $C_a + C_d, C_m$.

4. Examples of specific diodes

In the examples below, the experimental characteristics of the diodes [7-10] were used. They and L_{m0} are listed in Table 1. The dimensions of antenna $a = b = \lambda/4$, $A = 4ab$ and $C_a = \varepsilon_0 \varepsilon_e A / (0.1\lambda) = 6.6 \cdot 10^{-14} \text{ F}$, $C_m = 10^{-11} \text{ F}$, $r_m = 0$ and also $\lambda = 3 \cdot 10^{-3} \text{ m}$ were taken. The diodes 1 and 2 are the Schottky ones. In the diodes 3 and 4, the tunneling contact between metals was used. This made it possible to put $r_s = 0$ in them, and Exp. (14) is simplified to $C_i^* = C_a + C_m$ for $C_d \ll C_a + C_m$. In the diodes 1–3, the bias voltage $V_{op} = 0$, in the diode 4 the voltage $|V_{op}| = 0.076 \text{ V}$ at the current $|I_{op}| = 1.1 \cdot 10^{-12} \text{ A}$.

Note that matching the inductance can be created by a coplanar stripline open-circuited stub. The diode 1 in the paper [7] operates with the inductance $1.2 \cdot 10^{-10} \text{ H}$ so created.

Fig. 3 shows the dependences of the matching coefficient η on the angle ν for the diode 1 and different inductances. In the maxima $\eta = 1$, and they are higher than the highest value of the ratio 0.45 powers in the receiver with this diode for the antenna with the initial tangential current [7].

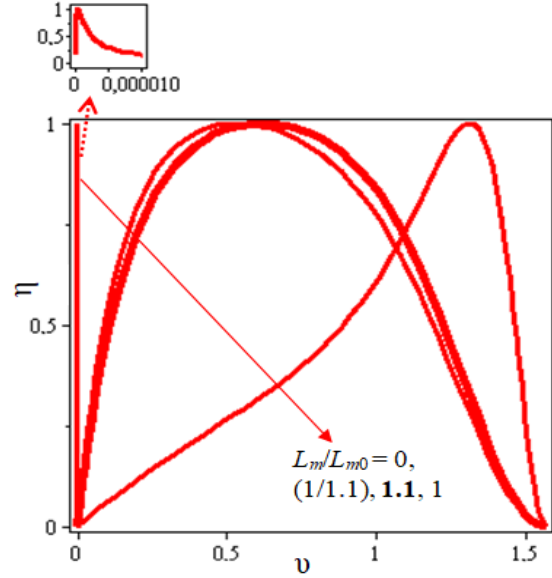


Fig. 3. Dependences of the coefficient of matching the radiation with the antenna load η (9) on the angle ν for the diode 1 and different inductances L_m . The characteristics of the diode are given in Table. At $L_m = L_{m0}$ (15), the reactive component $B = 0$. In the inset at the top, the beginning of the η dependence on L_m for $L_m = 0$ is shown.

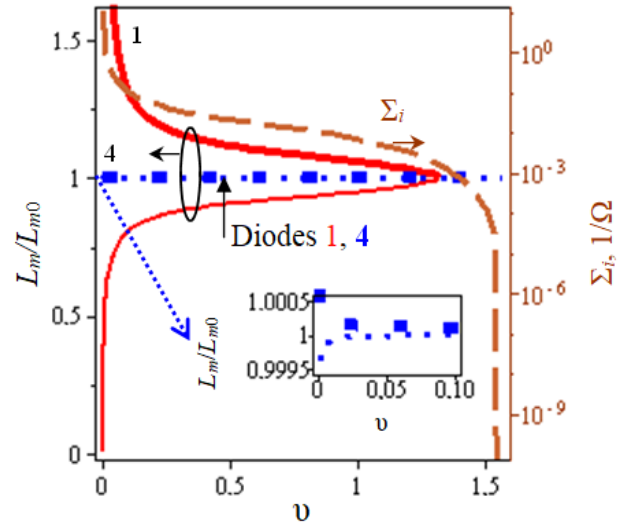


Fig. 4. Inductances L_m and angles ν for which $\eta = 1$. Each angle corresponds to two values L_m . In the inset, the beginning of the dependence of L_m on ν with the diode 4 is shown. The conductivity Σ_i for the values used in plotting Fig. 2, $b = a$.

In Fig. 4, solid lines show the values L_m and ν , at which $\eta = 1$ for the diode 1, and dot lines show this for the diode 4. Two values of the inductance L_m correspond to each angle ν . They are shown by lines of the same type but of different thicknesses. The dashed line shows the radiation conductivity Σ_i .

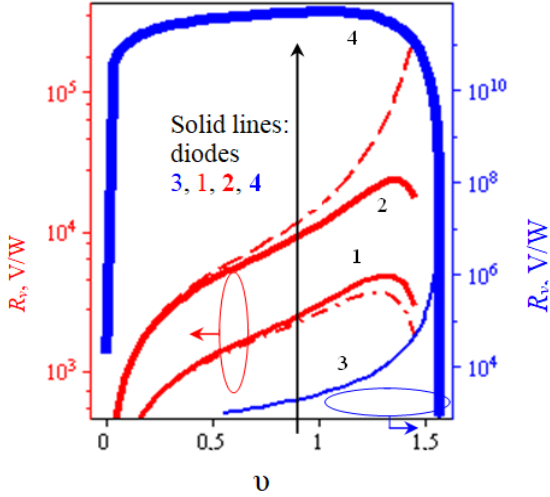


Fig. 5. Solid lines are the dependences of responsivities inherent to the receivers R_v for the diodes 1, 2, 3 and 4 on the angle ν and inductances $L_m = L_{m0}$. The dashed-dotted line indicates a decrease in R_v , if the inductance with active resistance $r_m = 0.19 \Omega$ is used for the diode 1. The dashed line in the figure shows an increase in R_v , under the assumption that the diode 2 has the intrinsic series resistance $r_s = 0$.

Now let's consider Fig. 5. On it, the solid lines represent the responsivity of receiver R_v with the diodes 1–4 and inductances $L_m = L_{m0}$. The rise of resistance r_d increases R_v . In the diodes 3 and 4, the resistance $r_s = 0$, and at the maxima $R_v = R_{vd}$.

In a mental experiment, the active resistance of the inductance operating with the diode 1 was taken equal $r_m = 0.19 \Omega$. The quality of the inductance $Q = L_{m0}\omega/r_m = 100$ corresponds to it. The loss in resistance r_m of part of the power incoming in the load reduces the receiver R_v . The dash-dotted line in the figure illustrates this.

In the second experiment, the resistance $r_s = 0$ was adopted for the diode 2. This increased the power in the active part of detector and R_v . The dashed line in the figure indicates this.

4.1. Minimal wavelength when matching and $r_s = 0$, $r_m = 0$

In the limiting case of resistances $r_s = 0$ and $r_m = 0$, quantities R_{vm} (12) and (13) are simplified to $R_{vm} = |\beta|r_d/G$ and $G = 1/r_d$, respectively, and $R_v = R_{vd} = |\beta|r_d^2$. R_v does not depend on the frequency to the smaller of frequencies $1/\tau_{\text{tun}}$ and $1/\tau_{\text{free}}$. Here, τ_{tun} and τ_{free} are the characteristic tunneling times and mean free paths of electrons in the metal, respectively. For the barrier 2.9 [10] estimated from the uncertainty relation for energy, the magnitude of $1/\tau_{\text{tun}}$ is of the order of 10^{15} Hz, while that of the frequency $1/\tau_{\text{free}}$ has the order of 10^{14} Hz [11], and the wavelength $3 \cdot 10^{-6}$ m corresponds to it.

Thus, the minimum wavelength of the device lies in the infrared range.

4.2. Noise equivalent power (NEP)

NEP equals to the power of the radiation incident on the antenna $\langle W_i \rangle$, at which $|V_{\text{res}}| = V_{\text{noise}}$. Here, V_{noise} is the noise voltage at the input of voltmeter measuring the response voltage. Noises of different nature create the voltage V_{noise} . Let us represent it, as the sum of the voltages of these noises, and estimate by the upper limit.

Table shows NEP for $V_{\text{noise}} = V_{\text{noise}}^{\text{John}} + V_{\text{noise}}^{\text{sh}}$, where $V_{\text{noise}}^{\text{John}} = 2\sqrt{k_B T_K r_d \Delta f}$ is the voltage of the thermal Johnson noise and $V_{\text{noise}}^{\text{sh}} = \sqrt{2qI_{\text{op}} \Delta f r_d}$ is the voltage of the diode shot noise [12]. Here, k_B , T_K , Δf and q are the Boltzmann constant, absolute temperature, the voltmeter bandwidth and electron charge, respectively.

A fluctuation in the number of thermal photons incident on the receiver increases V_{noise} [12]. Let us take this into account by adding the term $V_{\text{noise}}^{\text{ph}}$. It was defined as follows.

Of the parts of receiver included before the detector, the antenna has the largest area. Fluctuation of the number of photons falling on it from the environment causes noises of the electric field normal to its surface and therefore the antenna charge $Q_{\text{noise}}^{\text{ph}}$, current into earth and, finally, voltage $V_{\text{noise}}^{\text{ph}}$. This voltage does not exceed $Q_{\text{noise}}^{\text{ph}}/C_t$, where $C_t = C_a + C_m + C_d$ is the sum of capacitances charged with the noise current. To estimate the order of the greatest $V_{\text{noise}}^{\text{ph}}$ value, let's accept $V_{\text{noise}}^{\text{ph}} = Q_{\text{noise}}^{\text{ph}}/C_t$ with $Q_{\text{noise}}^{\text{ph}} = \epsilon_0 \epsilon_e E_{\text{noise}}^{\text{ph}} A$, where $E_{\text{noise}}^{\text{ph}}$ is the noise of electric field.

Let's denote as N the number of photons with a fixed energy of single photon, which are incident onto this antenna within a small time interval Δt . The expression for the time-averaged square of fluctuations of the $N/\Delta t$ rate was derived in the book [12]. The insertion of energy into it and integration over the energy gives the root-mean-square fluctuation of the energy flux $\langle W_{\text{noise}} \rangle$. Let's write down $\langle W_{\text{noise}} \rangle = \epsilon_0 \epsilon_e (E_{\text{noise}}^{\text{ph}})^2 \cdot (c/\sqrt{\epsilon_e \mu_e}) \cdot A$. From the above expressions at $\Delta t = 1/\Delta f$, the estimated formula $V_{\text{noise}}^{\text{ph}} = (30^{3/4} \pi^{5/4}/15) \epsilon_0^{1/2} \mu_e^{1/4} (\epsilon_e A)^{3/4} (k_B T_K)^{5/4} \Delta f^{1/4} / (ch_{pl}^{3/4} C_t)$ follows, where h_{pl} is the Planck constant.

The noise equivalent power values NEP_{ph} , in which $V_{\text{noise}} = V_{\text{noise}}^{\text{John}} + V_{\text{noise}}^{\text{sh}} + V_{\text{noise}}^{\text{ph}}$, are shown in Table. Both NEP and NEP_{ph} are calculated for $\Delta f = 1$ Hz, and their results are expressed in units [W]. The noise equivalent powers can be orders of magnitude smaller than those of receivers operating with antennas having a tangential initial current (see, for example, $\text{NEP} = 1.2 \cdot 10^{-12} \text{ W/Hz}^{1/2}$ [7]).

5. Conclusion

Generation of the initial current normal to the surface of antenna by electromagnetic waves has been discussed. The model of direct quadratic detection of the input signal in the stationary mode by a diode included in the load has been constructed.

Acknowledgments

The author is thankful to Prof. F. Sizov for support and fruitful discussions, Dr. G. Kilchynska for ongoing support.

References

1. Balanis C.A. *Antenna Theory*. New York: Wiley, 2005.
2. Rostami A., Rasooli H., Baghban H. *Terahertz Technology. Fundamentals and Applications*. Berlin: Springer, 2011.
3. Sizov F.F. *Detectors and Sources for THz and IR*. Millersville, USA: Materials Research Forum LLC, 2020.
4. Born M., Wolf E. *Principles of Optics*. 4th ed. London: Pergamon Press, 1970.
5. Jackson J.D. *Classical Electrodynamics*. New York: Wiley, 1962.
6. Smythe W.R. *Static and Dynamic Electricity*. 2th ed. New York: McGraw-Hill Book Company, 1950.
7. Brown E.R., Young A.C., Zimmerman J., Kazemi H., Gossard A.C. Advances in Schottky rectifier performance. *IEEE Microwave Mag.* 2007. **8**, No 3. P. 54–59. <https://doi.org/10.1109/MMW.2007.365059>.
8. Shashkin V.I., Murel A.V., Vostokov N.V. Parameters of microwave detectors on the basis of low-barrier Mott diodes for matrix radio-vision systems. *Zhurnal Radioelektroniki (Journal of Radio Electronics)*. 2013. No 8. P. 1–14 (in Russian).
9. Rakos B., Yang H., Bean J.A., Bernstein G.H., Fay P., Csurgay A.I., Porod W. Investigation of antenna-coupled MOM diodes for infrared sensor applications. In: Saraniti M., Ravaioli U. (eds) *Nonequilibrium Carrier Dynamics in Semiconductors. Springer Proceedings in Physics*, vol. 110. Berlin, Heidelberg: Springer, 2006. https://doi.org/10.1007/978-3-540-36588-4_23.
10. Choi K., Yesilkoy F., Chryssis A., Dagenais M., Peckerar M. New process development for planar-type CIC tunneling diodes. *IEEE Electron Device Lett.* 2010. **31**, No 8. P. 809–811. <https://doi.org/10.1109/LED.2010.2049637>.
11. Ashcroft N.W., Mermin N.D. *Solid State Physics*. Orlando, FL: Saunders College Publishing, 1976.
12. Jamieson J.A., McFee R.H., Plass G.N., Grube R.H., Richards R.G. *Infrared Physics and Engineering*. New York: McGraw-Hill Book Company, 1963.

Генерація струму, нормального до поверхні антени, електромагнітними хвилями та його застосування у високочутливому приймачі

В.Н. Добровольський

Анотація. Розглянуто генерування початкового струму, нормального до поверхні антени, електромагнітними хвилями. Показано, що кут ковзання (або падіння) хвилі з електричним вектором у площині, нормальним до поверхні, змінює опір випромінювання у широкому діапазоні його значень. Ця властивість дозволяє узгоджувати імпеданси випромінювання та навантаження. Пропонується використовувати цю властивість для створення високочутливого приймача випромінювання. У зв'язку з цим завданням побудовано модель детектування вхідного сигналу випромінювання квадратичним детектором прямого детектування в стаціонарному режимі з діодом, включеним як навантаження. Отримані результати доводять, що діод з високим диференціальним опором може ефективно працювати з антеною. Підвищення опору збільшує напругу відгуку детектора, його чутливість і зменшує еквівалентну шумову потужність приймача випромінювання. Можливе вдосконалення цих характеристик на порядки. Розглянутий механізм може бути застосований до детекторів інфрачервоного діапазону спектра, і збільшення довжини хвилі, в принципі, не обмежує його функціонування.

Ключові слова: узгодження імпедансів випромінювання та навантаження, квадратичний детектор, низька еквівалентна шумова потужність, діод Шоттки.